Ab Initio Molar Volumes and Gaussian Radii

Drew F. Parsons* and Barry W. Ninham

Research School of Physical Sciences and Engineering, Australian National University, Canberra, ACT 0200, Australia

Received: April 6, 2008; Revised Manuscript Received: November 27, 2008

Ab initio molar volumes are calculated and used to derive radii for ions and neutral molecules using a spatially diffuse model of the electron distribution with Gaussian spread. The Gaussian radii obtained can be used for computation of nonelectrostatic ion−ion dispersion forces that underlie Hofmeister specific ion effects. Equivalent hard-sphere radii are also derived, and these are in reasonable agreement with crystalline ionic radii. The Born electrostatic self-energy is derived for a Gaussian model of the electronic charge distribution. It is shown that the ionic volumes used in electrostatic calculations of strongly hydrated cosmotropic ions ought best to include the first hydration shell. Ionic volumes for weakly hydrated chaotropic metal cations should exclude electron overlap (in electrostatic calculations). Spherical radii are calculated as well as nonisotropic ellipsoidal radii for nonspherical ions, via their nonisotropic static polarizability tensors.

1. Introduction

An explanation of ion-specific effects categorized by Hofmeister series remains a key problem. Recently, it has become clear that the proper inclusion of quantum mechanical ionic dispersion interactions, missing from classical theories of electrolytes, lies at the heart of the phenomena.[1−3] The calculation and specificity of such forces, in either the continuum solvent approximation or extensions to include solvent structure, requires ionic polarizabilities, their frequency dependencies, and ionic radii consistent with electronic polarization cloud distributions. Ion-specific effects appear even at the cruder level of purely electrostatic theories that omit dispersion interactions. They do so there via ionic radii specific to each ion.

Indeed, Cheng et al. have identified that ion size plays a key role in ionic surface activity.[4,5] Anion affinities for the air−water interface, measured by electrospray ionization mass spectrometry, show a strong linear relationship between anion affinity and anion radius. The relationship between anion affinity and anion polarizability, on the other hand, is much less direct. To adequately study ion-specific effects, it is therefore crucial that ion size be correctly determined.

In developing electrolyte theory, the first and simplest entity that appears is the Born electrostatic self-energy for an ion with charge Q and hard-sphere radius a_s in a solvent with dielectric constant ε_0:

$$U_{el} = -\frac{Q^2}{2a_s\varepsilon_0} \tag{1}$$

In some studies, this formula is used to determine an effective ion radius for a given self-energy, defined experimentally or theoretically. For instance, Hummer, Pratt, and García[6] calculate a temperature-dependent self-energy from energy fluctuations, corresponding to the second cumulant of an expansion of the average Boltzmann factor of the electrostatic interactions between an ion and an SPC/E partial charge model of water. By fitting the ion radius a_s in eq 1 against the calculated cumulant, they propose that a temperature-dependent radius $a_s(T)$ may be extracted. The temperature dependence of the self-energy arises through the interaction of the ionic charge with the solvent partial charges and through solvent−solvent interactions. Solvent−solvent interactions may be assigned to a temperature-dependent dielectric constant $\varepsilon_0(T)$, and therefore any temperature dependence in the ion radius would be largely due to ion−solvent interactions. However, the dielectric constant is relatively independent of temperature, with the value for water varying by only 1% between 0 and 100 °C, indicating a low temperature dependence in energy fluctuations due to solvent−solvent interactions. It seems reasonable to expect that ion−solvent interactions would similarly yield a relatively mild temperature dependence. Hence, in this Article, we treat ion radius as a constant independent of temperature, while the solvent dielectric constant is fixed at $T = 25$ °C.

Other studies in the theory of electrolytes[7,8] have used Pauling[9] or Gourary−Adrian[10] ionic radii. These are derived from interionic distances (Pauling), or from electron density minima (Gourary−Adrian), determined from X-ray diffraction of salt crystals. Problems with the use of these radii are well documented. Pauling's radii involve a nonelectrostatic repulsion term but neglect nonelectrostatic attraction (dispersion forces) in the crystal. Crystallographic measurements depend on the coordination number of the ion in the given crystal, which may vary depending on the counterion. This leads to varying estimates of the crystalline ionic radius. Marcus[11] derived a set of ionic radii extracted from the theory of liquids rather than from solid-state theory. He estimated ionic radii from ion−water distances taken from pair correlation functions determined from X-ray or neutron scattering or from computer simulation. Thus, the hard-sphere radii so obtained change depending on the ion pair of the crystal or electrolyte on which the diffraction experiment is performed. For instance, the estimate of a halide ion radius varies depending on the cation with which it is paired.[12] This variation can be understood by taking a quantum mechanical view of the ion. The excess charge is spatially dispersed in a diffuse electron cloud rather than located on the surface of a hard sphere. A deviation in ionic radius determined by crystallographic nuclear separations is therefore to be

* Corresponding author. E-mail: drew.parsons@anu.edu.au.

10.1021/jp802984b CCC: $40.75
Published on Web 01/13/2009

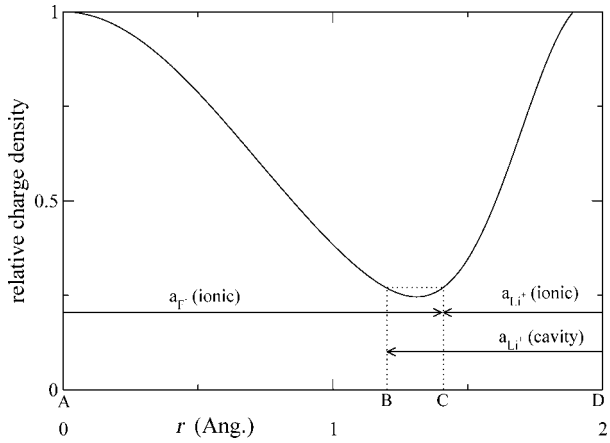

Figure 1. The Rashin−Honig scheme for determining cationic hard-sphere cavity radii.[13] The anion (F^-) is at point A; the cation (Li^+) is at point D. The crystal anionic radius is length AC. The crystal cationic radius is length CD. Rashin and Honig's cavity radius for the cation is length BD, where the electron density near the anion has risen to the same level as point C (where the anionic radius intersects the cationic electron density).

expected. It occurs, for example, due to varying degrees of overlap between the electron clouds of cation and anion.

Rashin and Honig[13] attempted to account for these changes in electron overlap by taking the cavity radius for metal cations, rather than intrinsic ionic radius, as the distance at which the electron density around the counterion starts to become significant. That is to say, with an anion (e.g., F^-) located at 0 (position A) in Figure 1 and a cation (e.g., Li^+) located at D, Rashin and Honig measured the electron density at point C, at a distance AC corresponding to the crystal ionic radius of the anion. The crystal ionic radius of the cation would be length CD, but Rashin and Honig take the cationic cavity radius to be distance BD. This is the point where the electron density near the anion becomes as strong as it was at point C where the anionic radius intersected the cationic electron cloud. However, although based on electron densities, this approach still yields a hard-sphere radius, which is in principle inconsistent with the quantum view of an ion with a diffuse electron cloud.

In considering the concept of ionic radius for ions in solution, it is necessary to go further and take into account the role of the ion's hydration shell. Collins[14,15] identifies two kinds of ions: at one extreme, cosmotropic ions, such as Li^+, F^-, have tightly bound hydration shells. At the other extreme, chaotropic ions have weakly bound hydration shells. Typical members of this class are Cs^+, Br^-. This distinction between hydrated and unhydrated radii is consonant with Rashin and Honig's idea of a cavity radius, which is distinct from the intrinsic ionic radius. This choice of different radii has consequences for calculations of electrostatic energies, as it affects the volume within which the charge is contained. This is explored further in section 8.

2. Dispersion Forces and Molecular Size

A complete quantum description of ion−ion interactions would include contributions from the permanent charge distribution as well as the charge fluctuations leading to nonelectrostatic dispersion forces. The dispersion forces considered here refer to induced dipole−induced dipole interactions. A third class of interaction would be induction forces, that is, interactions between the permanent charge and induced dipole. Induction forces are implicated in solvent effects such as a reduction of the polarizability of an ion in solution as compared to gas phase[16] and, together with dispersion forces, play a role in the disruption of the molecular water network in ionic hydration shells.[17] The dispersion forces considered in this section have been developed[18−22] by applying the Lifshitz theory to the electromagnetic field of a polarizable particle, describing by its polarizability $\alpha(i\omega)$ without consideration of its permanent charge. Induction forces are included at the same level of semiclassical Lifshitz theory by adding the permanent charge distribution alongside the induced dipole at the entry point of the theory (Maxwell's equations); however; this theoretical development is beyond the scope of the current Article. The relative magnitude of induction energies may, however, be compared to dispersion and electrostatic energies by considering zero-frequency contributions to the self-energies in vacuum. The induction self-energy for an ion with charge Q, radius a, and static polarizability α_0 is approximately $U_{ind} = -Q^2\alpha_0/2a^4$ (cf., charge-induced dipole interaction energy),[23] while the dispersion self-energy is given below, eq 3. The induction self-energies for Na, K, Cl, Br in vacuum are −12.5, −56.1, −357.0, −201.4 kJ mol^{-1}, respectively, while dispersion self-energies in vacuum are 1913.1, 1359.8, 569.6, 410.3 kJ mol^{-1}, respectively. That is, the magnitude of induction self-energies may vary between 1% and 60% of the magnitude of dispersion self-energies.

The usual theory of dispersion forces for point molecules assumes a separation between the electrostatic (permanent charge with hard core repulsion) and nonelectrostatic (polarization charge). Given that assumption, extensions of the theory to include molecular size have also been developed.[18−22] A semiclassical spatially diffuse approximation to the polarizability can be extracted from the full quantum mechanical expression for the polarization density. It is applicable equally to ions with a spherically symmetric Gaussian distribution:

$$\alpha(\vec{r},\omega) = \alpha(\omega)\frac{\exp(-r^2/a_g^2)}{\pi\sqrt{\pi}a_g^3} \tag{2}$$

of the spatial polarizability distribution with Gaussian radius a_g. Semiclassical Lifshitz theory itself has been proven successful, for instance, in correctly describing the Lamb shift.[19] The Gaussian spatial distribution may be justified from the 1s ground-state wave function.[24,25] More sophisticated spatial distributions based on a wider set of wave functions have been studied,[26,27] leading Lu and Marlow[27] to suggest the use of an exponential spread. Schmidt and McKinley, however, recommend a Gaussian spatial distribution in favor over an exponential (Slater-type) distribution.[25] Moreover, the Gaussian model is convenient for us because it is more readily extended to nonspherical ions (see section 9) than other models.

With such a distribution to characterize finite size, one can derive a dispersion self-energy that is the analogue of, and additional to, the electrostatic Born self-energy of an ion. The dispersion self-energy at temperature T in a solvent with frequency-dependent dielectric function $\varepsilon(i\omega)$ is given in the nonretarded limit by

$$U_{ds} = \frac{4kT}{\sqrt{\pi}a_g^3}\sum_{n=0'}^{\infty}\frac{\alpha(i\omega_n)}{\varepsilon(i\omega_n)} \tag{3}$$

where the prime in $n = 0'$ indicates that the zero frequency term is taken with a factor of 1/2. The temperature-dependent modal frequencies are as usual $\omega_n = 2\pi kTn/\hbar$. The full expression for the dispersion self-energy includes retardation and gives an excellent semiclassical result for the Lamb shift; that is, the semiclassical theory for the polarization is a reasonable approximation.[19] The ion-specific character of the

dispersion self-energy is evident not only in the dynamic polarizability $\alpha(i\omega)$ but also in the Gaussian radius a_g. Clearly, an inconsistency will arise if a hard-sphere ionic radius a_s is used in place of the diffuse Gaussian radius a_g.

A complication often avoided with the concept of an effective ionic radius is the approximation that an ion can be treated as if spherical, characterized to good enough approximation by a single radius (whether hard-sphere or Gaussian distribution). Yet complex ions are certainly not spherical. Nitrate (NO_3^-), for example, is planar, as is chlorate (ClO_3^-). We here argue that it may be more appropriate to characterize ionic size in terms of volume rather than by radius. We therefore address the question of defining ionic volumes in parallel with the question of determining effective Gaussian radii.

The aim of this Article then is to present a consistent method for determining Gaussian radii that describe the spatial spread of the electron and polarization clouds for both ions and neutral molecules. Ionic volumes are determined by ab initio quantum calculations and mapped back onto a Gaussian model of the electron cloud. The effects of these different Gaussian radii on physical characteristics are compared to those with an equivalent hard-sphere radius, using the electrostatic self-energy (Born energy) of both models for comparison. The method is generalized to the case of nonspherical ions, yielding sets of three nonisotropic spheroidal Gaussian radii.

Calculations are performed for a comprehensive set of simple and complex ions of relevance to specific ion effects. We have also included a small number of molecules of biological interest. These are formamide (neutral molecule) as the simplest amide, glycine (zwitterionic) as the simplest amino acid, ammonia, ethanolamine (as the protonated cation), and choline. Because the presence of dissolved gas has been implicated in discussions of long-range hydrophobic forces,[28−32] we also include the gas molecules O_2, N_2, and CO_2.

3. Electron Density: Gaussian Model

The ionic polarizability derives from the response of the ionic electron cloud to an external electric field. It seems reasonable then to accept a model of the spatial structure of the ionic (or molecular) charge distribution $\rho(\vec{r})$ that matches the spatially dispersed model used for the polarization density $\alpha(\vec{r}, \omega)$ (cf., eq 2), that is

$$\alpha(\vec{r}, \omega) = \alpha(\omega)\rho(\vec{r}) \tag{4}$$

where $\alpha(\omega)$ is the dynamic polarizability. The charge distribution is normalized by $\int d^3\vec{r}\rho(\vec{r}) = 1$. The excess charge density $q(\vec{r})$ of an ion with charge Q would then be $q(\vec{r}) = Q\rho(\vec{r})$.

We therefore propose, referring to the Gaussian spatial model of the polarizability, eq 2, to model the ionic charge distribution as

$$\rho(\vec{r}) = \frac{1}{V_g}\exp\left(\frac{-r^2}{a_g^2}\right) \tag{5}$$

V_g describes the ionic (or molecular) volume, that is, the volume within which the probability of finding the ion's electrons is 1. For the Gaussian model, $V_g = \pi(\sqrt{\pi})^{1/2}a_g{}^3$.

By assigning a meaning to ionic or molecular volume in this manner, we are able to establish a correspondence between the diffuse ionic Gaussian radius a_g defined above and the conventional hard-sphere radius a_s. The charge distribution of the hard sphere is $\rho(\vec{r}) = \delta(|r| < a_s)/V_s$ (or $\delta(|r| = a_s)$ for Born's original charged shell)[33] with $V_s = 4\pi a_s^3/3$, the volume of the hard sphere. For a given Gaussian radius, the equivalent hard-sphere radius may be determined by simply conserving the ionic volume, $V_s = V_g$. Hence,

$$a_s = a_g\left(\frac{3\sqrt{\pi}}{4}\right)^{1/3} \tag{6}$$

Equating the Gaussian and hard-sphere volumes underlines the notion mentioned above that the fundamental unit of molecular size is volume, not radius. By presenting data such as self-energy in terms of volume, the question of whether it is more appropriate to characterize the data using a Gaussian radius or hard-sphere radius is in a sense avoided and treats nonspherical ions in a more meaningful manner.

4. Ionic and Molecular Volume

The question then becomes, how best can one assign a volume to ions or neutral molecules? One approach is to use experimental densities, of the solid salt, say, to derive molar volumes, $V_m = M/\rho$. ρ here refers to macroscopic material density and M to molar mass. This approach is problematic, particularly for determining the volume of individual ions. It is problematic for precisely the same reasons already mentioned, that the volume per ion depends on the forces of interactions between ions. Use of the density of the solid salt would require subtraction of the volume of the counterion, leading to a bootstrapping problem. It could only be resolved by starting with predetermined hard-sphere ionic radii (Pauling, for instance, artificially assigned a value of 0.6 Å to the ionic radius of Li^+).[9] This would introduce the contradiction already discussed of forcing a fit of the extent of a diffuse electron cloud to a hard-sphere contact radius. The seriousness of this contradiction may be ameliorated by equating hard sphere and diffuse volumes as remarked in the previous section. Yet other problems remain. If the density of a solid salt is used in this way, what real relationship do the resulting individual ionic volumes so extracted have to the volume of the electron cloud of an individual ion in solution? Moreover, experimental densities are not available for all molecules and salts of interest in the context of Hofmeister specific ion effects and dispersion interactions. This in part too is because of residual hydration.

In the circumstances, the only way forward seems to lie in appeal to ab initio quantum mechanics. Quantum chemical software including Gaussian[34] does have the functionality of estimating molecular volumes based on the electron cloud of the molecule (keyword Volume in Gaussian). We propose therefore to use these ab initio volumes and extract Gaussian radii from them. The calculation implemented by the Gaussian program defines molecular volume as the space inside an isodensity surface of $\rho_0 = 0.001$ electrons/Bohr^3 (0.067 electron/Å^3). This is essentially another hard-sphere volume; beyond this volume there is "no more" electron density, and hence we refer to this volume as the exclusive volume V_{ex}. It permits no overlap between neighboring ions or molecules. We reconcile this hard-sphere volume with the diffuse charge distribution of eq 5 by taking ρ_0 to be the charge density at distance a_{ex}, the hard-sphere radius corresponding to the exclusive volume V_{ex}. This then enables us to determine the Gaussian radius using the ab initio exclusive volume, by solving the transcendental equation for a_g,

$$\rho(a_{ex}) = \frac{\exp(-a_{ex}^2/a_g^2)}{\pi\sqrt{\pi}a_g^3} = \rho_0 = 0.001 \tag{7}$$

In general, there will be two solutions near a_{ex}. We take the smaller value (which is always less than a_{ex}; the larger solution

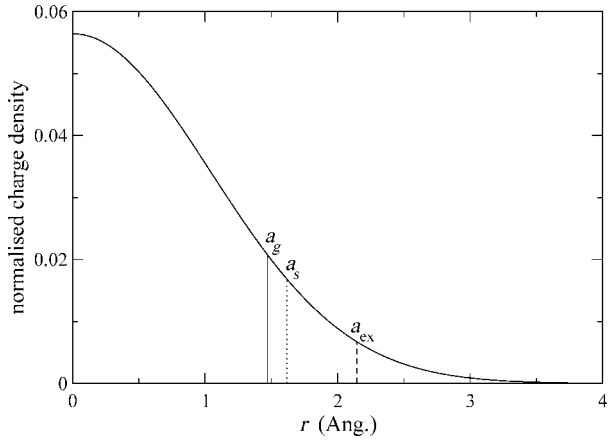

Figure 2. Schematic of ionic charge density as a function of distance from ion center, comparing the Gaussian radius a_g against the equivalent hard-sphere radius a_s (conserving total volume), which allows for electron cloud overlap. The exclusive hard-sphere radius a_{ex} corresponding to the ab initio exclusive volume, allowing no (or little) overlap, is also marked. The sample radii here are for Cs^+.

may sometimes be greater than a_{ex}, which is unphysical. It contradicts the notion of a_{ex} being the largest distance beyond which there is "no further" electron density).

Depending on the ab initio exclusive volume, there may be no solution to the equality in eq 7. In these situations, we employ a least-squares approach, selecting a_g to minimize $[\rho(a_{ex}) - \rho_0]^2$.

Once a_g is determined in this way, we have the Gaussian volume $V_g = \pi(\sqrt{\pi})^{1/2}a_g^3$, which we interpret as the actual ionic or molecular volume for the diffuse charge distribution. The equivalent hard-sphere radius is a_s. While a_{ex} is the exclusive hard-sphere radius that allows for no (or little) overlap of electron clouds, a_s is a "soft" hard-sphere radius that does include overlap; see Figure 2.

5. Details of Computational Procedures

Ab initio volume calculations are implemented in Gaussian using numerical Monte Carlo integration. This introduces a fairly large degree of error; therefore, we use keywords SCF=Tight Volume=Tight and repeat the volume calculation 100 times for each ion or molecule to reduce random error. Because of the error, we test for an equality solution to eq 7 at the limits of the error bars of V_{ex} before turning to the least-squares solution. That is, we solve eq 7 for a_g first using the average exclusive volume V_{ex}, accepting this solution if it exists. If it does not, we solve the equality using volumes $V_{ex} - \Delta V$ and $V_{ex} + \Delta V$, where ΔV is the error in V_{ex}. If both of these volumes provide a solution, then we take the average, otherwise we accept the single solution for a_g. Finally, if none of the equalities for the three volumes yields a solution, then we accept the least-squares solution based on V_{ex}.

For volume calculations, we use ab initio basis sets similar to those required to calculate accurate polarizabilities. This requires basis sets augmented with diffuse functions. The aug-cc-* series of basis sets[35,36] have been found satisfactory.[37,38] Given the number of repetitions of the volume calculation required, we use the faster aug-cc-pVDZ basis, rather than, say, the more accurate aug-cc-pVQZ. Any difference in volume between these basis sets would be well within the random error of the Monte Carlo integration. aug-cc-* is not available for the larger alkali and alkali earth metals. For these ions, we use the ECPnMDF basis set (and pseudopotential).[39,40] Standard quantum chemical geometry optimizations (minimizing energy) were performed first before undertaking the volume and polarizability calculations.

Calculations are performed at a Hartree−Fock (HF) level of theory, for consistency with dynamic polarizability calculations of $\alpha(i\omega)$ over imaginary frequencies.[37] These calculations use the Effective Fragment Potential method,[41] which is incompatible with higher methods incorporating electron correlations such as Møller−Plesset (e.g., MP2) or coupled-cluster (e.g., CCSD(T)). The difference in polarizability between calculations using HF and electron correlations is not extreme for most of the closed shell ions and molecules considered here. The electron correlation correction to the polarizability of Cl^-, for instance, is around 17%.[42] In any case, electron correlation has no significant impact on ion volumes, which are the chief subject of the present Article. For example, the volume of Cl^- is 29.9 ± 2.7 cm^3/mol under HF, and 28.3 ± 2.4 cm^3/mol under MP2, exactly identical within error bounds.

The oxygen gas molecule needs special mention. We have included the normal triplet state (multiplicity 3), which has an open shell electronic structure, as well as the exotic closed shell singlet state (multiplicity 1). Ab initio dynamic polarizabilities are currently only available for closed shell molecules,[37] hence the need for the latter oxygen state. However, in the case of the oxygen triplet state, the static polarizability is 1.461 and 1.422 $Å^3$ at HF and CCSD(T) levels of theory, respectively, justifying the use of Hartree−Fock calculations for the triplet state. Moreover, the static polarizability of the singlet state is 1.426 $Å^3$, so using it rather than the triplet state for dynamic polarizability calculations is reasonable.

We note that there is a strong solvation effect on ion polarizabilities. The gas-phase static polarizability of Cl^- is 5.5 $Å^3$ (with electron correlation),[42] but Car−Parrinello molecular dynamics calculations of the chloride in solution reduce the polarizability down to 4 $Å^3$,[16] a reduction of around 25%. Nevertheless, while the effect of the solvation environment on the polarizability of the electron cloud is significant, it seems plausible that its effect on intrinsic ion volume will be smaller. Ion solvation using quantum chemical electron structure calculations has been studied[43−48] but is out of the scope for this Article. The relationship of solvation shell to ion size is addressed at a phenomenological level in section 8.

6. Molar Volumes and Gaussian Radii

Because the Gaussian model of eq 5 is a spherically symmetric distribution, the procedure for determining a_g makes best sense for spherical ions and molecules (although the ab initio volume*s* of nonspherical ions and molecules are still valid). We therefore collect the ab initio exclusive volumes V_{ex} for spherical ions in Table 1 along with the Gaussian radius a_g calculated from it. For reference, we also list the exclusive hard-sphere radius a_{ex}, the Gaussian molar volume V_g derived from a_g, and the equivalent overlapped hard-sphere radius a_s of the ion or molecule. Experimental crystalline ionic radii (at their smallest available coordination number)[49] for simple atomic ions are presented in the table for comparison. The crystalline radii agree reasonably well with our equivalent hard-sphere radii with an average discrepancy of 0.2 Å (typically about 15%), in some cases matching exactly. Oxide gives the strongest discrepancy, with an equivalent hard-sphere radius of 2.14 Å but crystalline ionic radius 1.21 Å at coordination number 2 (or 1.40 Å at coordination number 6).

Because the theory of ionic and molecular interactions between nonspherical ions and molecules is not yet well developed, we list equivalent volumes and mean spherical radii

TABLE 1: Static Polarizabilities α_0 and Gaussian Radii a_g for Spherical Ions[a]

ion	α_0 (Å^3)	a_g (Å)	V_g (cm^3/mol)	a_s (Å)	a_{crys} (Å)	V_{ex} (cm^3/mol)	a_{ex} (Å)
F^-	1.218	1.02	3.5	1.12	1.33	15.4 ± 0.9	1.83
Cl^-	4.220	1.69	16.3	1.86	1.81	29.9 ± 2.7	2.28
Br^-	6.028	1.97	25.6	2.16	1.96	35.3 ± 3.2	2.41
I^-	8.967	2.12	32.0	2.33	2.20	44.2 ± 4.6	2.60
Li^+	0.028	0.38	0.2	0.42	0.59	2.2 ± 0.9	0.95
Na^+	0.131	0.61	0.8	0.67	0.99	5.9 ± 2.0	1.33
K^+	0.795	0.96	3.0	1.06	1.37	14.0 ± 3.9	1.77
Rb^+	1.348	1.12	4.7	1.23	1.52	17.9 ± 4.9	1.92
Cs^+	2.354	1.47	10.7	1.62	1.67	24.8 ± 6.1	2.14
Fr^+	2.938	1.44	10.1	1.59	1.80	28.1 ± 3.7	2.23
Be^{2+}	0.0075	0.28	0.08	0.31	0.27	1.1 ± 0.5	0.75
Mg^{2+}	0.068	0.50	0.4	0.55	0.57	4.0 ± 1.4	1.16
Ca^{2+}	0.475	0.80	1.7	0.88	1.00	10.1 ± 2.6	1.59
Sr^{2+}	0.859	0.96	3.0	1.05	1.18	14.0 ± 3.8	1.77
Ba^{2+}	1.567	1.21	5.9	1.33	1.35	19.9 ± 4.8	1.99
Ra^{2+}	1.982	1.35	8.3	1.49	1.48	22.8 ± 3.1	2.08
oxide O^{2-}	4.359	1.95	24.7	2.14	1.21	34.2 ± 1.3	2.38
perchlorate	4.790	2.17	34.4	2.39		47.5 ± 3.1	2.66
sulfate	6.132	2.29	40.5	2.52		56.0 ± 3.9	2.81
phosphate	9.891	2.40	46.2	2.64		63.8 ± 4.2	2.94
arsenate	11.430	2.44	48.7	2.68		67.4 ± 4.8	2.99
ammonium	1.278	1.09	4.4	1.20		17.2 ± 1.2	1.90
Me_4N^+	7.448	2.47	50.8	2.72		70.2 ± 3.9	3.03

[a] V_g is the corresponding gaussian molar volume, and a_s is the equivalent hard-sphere radius (including electron overlap). a_{crys} is the experimental crystalline ionic radius (at smallest coordination number).[49] V_{ex} is the ab initio exclusive molar volume with no electron overlap; a_{ex} is the corresponding exclusive hard-sphere radius. Me_4N^+ refers to tetramethylammonium.

TABLE 2: Mean Isotropic Static Polarizabilities α_0 and Mean Spherical Gaussian Radii a_g for Nonspherical Ions and Molecules[a]

ion/molecule	α_0 (Å^3)	a_g (Å)	V_g (cm^3/mol)	a_s (Å)	V_{ex} (cm^3/mol)	a_{ex} (Å)
hydronium H_3O^+	0.882	0.97	3.1	1.07	14.4 ± 1.1	1.79
hydroxide	2.746	1.26	6.7	1.38	21.0 ± 1.2	2.03
nitrate	4.008	2.01	27.3	2.21	37.8 ± 2.3	2.46
cyanide	3.915	1.89	22.6	2.08	31.3 ± 2.0	2.32
thiocyanate	7.428	2.18	34.6	2.39	47.8 ± 4.1	2.67
triflate $CF_3SO_3^-$	6.402	2.44	48.7	2.68	67.3 ± 4.2	2.99
chlorate	5.488	2.14	32.7	2.35	45.2 ± 3.0	2.62
carbonate	6.043	2.13	32.6	2.35	45.0 ± 2.5	2.61
bicarbonate	4.177	2.06	29.1	2.26	40.2 ± 2.6	2.52
hydrogen sulfate	5.089	2.22	36.9	2.45	51.0 ± 3.9	2.72
hydrogen phosphate	6.846	2.32	42.0	2.55	58.0 ± 4.4	2.84
dihydrogen phosphate	5.470	2.26	38.9	2.49	53.8 ± 3.7	2.77
hydrogen arsenate	7.946	2.38	45.5	2.62	62.9 ± 4.2	2.92
dihydrogen arsenate	6.378	2.33	42.6	2.57	58.9 ± 4.7	2.86
cacodylate	9.633	2.54	55.2	2.80	76.2 ± 5.3	3.11
formate	3.937	1.96	25.4	2.16	35.1 ± 2.3	2.40
acetate	5.607	2.20	35.5	2.41	49.0 ± 2.7	2.69
tartrate	11.135	2.75	70.1	3.03	96.8 ± 4.3	3.37
citrate	16.051	3.02	92.1	3.32	127.2 ± 5.1	3.69
water	1.230	1.04	3.7	1.14	15.9 ± 1.1	1.85
ammonia	1.880	1.23	6.2	1.35	20.3 ± 1.5	2.00
formamide	3.614	1.97	25.5	2.16	35.2 ± 2.3	2.41
ethanolamine−H^+	5.042	2.22	36.9	2.45	51.0 ± 2.5	2.72
glycine±	5.812	2.26	38.8	2.49	53.6 ± 3.0	2.77
choline	9.621	2.69	65.1	2.96	90.0 ± 4.7	3.29
N_2	1.650	1.28	7.1	1.41	21.5 ± 1.6	2.04
O_2 (triplet)	1.461	1.18	5.6	1.30	19.4 ± 1.3	1.97
O_2 (singlet)	1.426	1.18	5.5	1.30	19.3 ± 1.2	1.97
CO_2	2.269	1.57	12.9	1.72	26.1 ± 2.2	2.18

[a] V_g is the corresponding gaussian molar volume, and a_s is the equivalent hard-sphere radius (including electron overlap). V_{ex} is the ab initio exclusive molar volume with no electron overlap; a_{ex} is the corresponding exclusive hard-sphere radius.

for nonspherical molecules in Table 2. For our purposes, a nonspherical ion or molecule is one with a nonisotropic polarizability tensor (ammonium, for instance, is "spherical" by this definition).

It is curious to note that the ionic volumes of protonated complex ions are, counterintuitively, smaller than the deprotonated species. For instance, carbonate CO_3^{2-} is found to have a Gaussian molar volume of 32.6 cm^3 mol^{-1}, while bicarbonate HCO_3^- has a volume of only 29.1 cm^3 mol^{-1}. This trend is consistent over all such samples, the sulfates, phosphates, and arsenates, with the dihydrogen anion of the latter two being again smaller than the first protonated anion. The trend is also

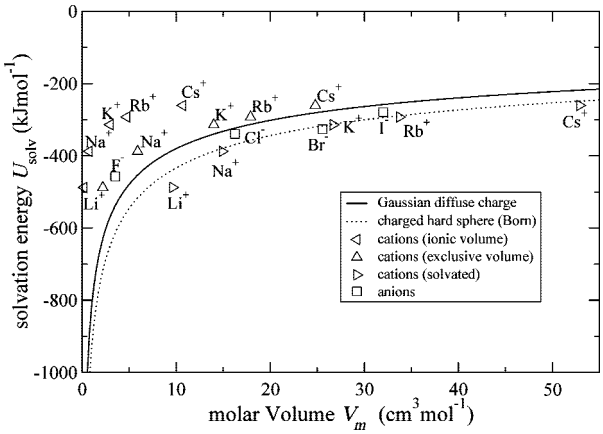

Figure 3. Electrostatic solvation energy (self-energy) of singly charged ions in water as a function of ionic volume. The solid curve represents the Gaussian diffuse model of the charge distribution; the dotted curve indicates the traditional hard-sphere Born model. For comparison, the experimental values of selected ions are also given. Three sets of cationic molar volumes are compared, based on (1) intrinsic radius, (2) exclusive radius (no electron overlap), and (3) adding a solvent layer.

true of ammonia as compared to ammonium, but is broken by water, which is slightly smaller than the hydronium ion H_3O^+.

Finally, for consistency with section 9 where static polarizability tensors of nonspherical ions are used, the mean isotropic static polarizabilities are listed in Tables 1 and 2. These are calculated at the Hartree−Fock level of theory using the aug-cc-pVQZ and other basis sets used to calculate dynamic polarizabilities[37] (whereas the faster aug-cc-pVDZ was used for volume calculations).

7. Application: Gaussian Electrostatic Self-Energy

The electrostatic self-energy for the charged Born hard sphere was given in eq 1. Applying instead a Gaussian charge distribution $q(\vec{r}) = Q\rho(\vec{r})$ (see eq 5), the electrostatic potential derived from Poisson's equation $\nabla^2\psi(\vec{r}) = -4\pi\rho(\vec{r})/\varepsilon_0$ is

$$\psi(r) = \frac{Q\ \mathrm{erf}(r/a_g)}{\varepsilon_0 r} \tag{8}$$

The Gaussian electrostatic self-energy $U_s = -{}^1/_2\int d^3r q(r)\psi(r)$ is then

$$U_s = \frac{Q^2}{\sqrt{2\pi}\varepsilon_0 a_g} \tag{9}$$

differing from the Born energy (eq 1) by a factor of $1/(\sqrt{2\pi})^{1/2} \approx 1/2.5$ rather than 1/2, which is about 20% smaller for the same radius.

We compare the Gaussian estimate with the equivalent Born hard-sphere electrostatic energy (using $a_s = a_g(3(\sqrt{\pi})^{1/2}/4)^{1/3}$) via the solvation energy U_{solv}, which is the difference in self-energy between solution and vacuum, $U_{solv} = U_s[\varepsilon_0] - U_s[\mathrm{vac}]$. The two solvation energies in water ($\varepsilon_0 = 78.12$) are shown in Figure 3 with selected ions marked. Experimental solvation energies are also shown for comparison. We see that the effect of the Gaussian model, even using equivalent spherical radii, is to reduce the solvation energy by around 10%.

We emphasize that the calculation here refers only to the electrostatic component of the self-energy. The full self-energy also includes a nonelectrostatic dispersion component (as well as ion−solvent interactions),[6,43] and complete agreement with experimental solvation energies is not expected without those components.

8. The Question of Solvated Ionic Radius

It is notable in Figure 3 that the experimental solvation energies of the halogen anions, apart from F^-, match reasonably well with the theoretical curves, whereas the experimental values for the alkali cations are far lower in magnitude than the theoretical electrostatic solvation energies using intrinsic ionic radii. Hence, the cavity effect of the cations' solvation shells is not accounted for.

A similar problem was addressed by Rashin and Honig.[13] They indicated, as mentioned in the Introduction, that a reasonable estimate of solvation cavity radius rather than intrinsic ionic radius of cations is given by the distance at which the electron density of the counterion (the anion) starts to rise. They justified the treatment of metal cations in this way, differently from the anions, by suggesting that the empty valence shell of the cation contributes to the cavity volume (but not to the intrinsic ionic volume). This indicates no or little overlap with the cationic electron cloud. This scenario matches the ab initio exclusive volumes, which we calculated at first. We therefore include the experimental solvation energies of cations plotted against exclusive volume in Figure 3. We find that assignment of these volumes does bring the metal cations much closer into line with the theoretical electrostatic solvation energies. We do not expect this approach, that is, adding the volume of the empty valence shell, will be relevant to complex organic cations such as tetramethylammonium or choline.

We can apply an alternative correction to the radii of our cations in solution by considering the solvated cation with a single layer of water molecules. The degree of overlap between the electron cloud of the cation and the water molecules is not known a priori without further computation of the solvated cluster system. It is not reasonable to simply add the Gaussian radii of cation and water molecule to determine the Gaussian radius of the solvated cation. However, we have already identified the equivalent hard-sphere radius a_s as a radius that allows for electron cloud overlap. It seems reasonable therefore to sum these radii, so that the hard-sphere radius (with overlap) of the solvated ion is $a_s^{solv} = a_s^{ion} + a_s^{water}$. Equivalent Gaussian radii of the solvated metal cations may be estimated by reversing eq 6. With solvation volumes calculated to match these radii, the positions of the experimental solvation energies of solvated cations are marked in Figure 3 and are also seen to line up with the theoretical curves.

The question of ion size with or without a water layer in the context of solvation effects has been introduced in Collin's explanation of the phenomenon of chaotropic (disrupting water structure) and cosmotropic (sustaining water structure) ions.[14,50] Collins' Law of Matching Water Affinities is a phenomenological rule that addresses the capacity of ions to form ion pairs in solution. It suggests that ion pair formation is governed by the "hydration strengths" of the ions, with cosmotropes pairing with other cosmotropes, and chaotropes with other chaotropes. Cosmotropic ions then are those ions that are tightly bound to their first solvation shell. Chaotropic ions are weakly bound to their first solvation shell. Invoking this distinction between cosmotrope and chaotrope, we could argue that strongly hydrated metal cations (cosmotropes) such as Li^+ or Na^+ should be treated using solvated ion volumes, as discussed in the preceding paragraph. Weakly hydrated metals cations (chaotropes) such as Cs^+ should be treated using their bare ionic volumes. Collins quantifies ion−water affinity via Jones−Dole

viscosity *B*-coefficients:[14,51] cosmotropes have positive while chaotropes have negative *B*-coefficients. Of the group I cations, Li^+ and Na^+ are cosmotropes (although Na^+ is borderline), and heavier cations (K^+, Rb^+, Cs^+) are chaotropes. H^+ has a positive *B*-coefficient; we assume therefore that the hydronium ion H_3O^+ is cosmotropic. The group II cations (Mg^{2+}, Ca^{2+}, Ba^{2+}, Sr^{2+}) are all cosmotropic. In general, multiply charged ions are cosmotropic when the ion is sufficiently small. It is not clear if this rule continues to apply to macroions such as charged protein molecules, but it remains valid[52] for the complex triply charged cation citrate, a known cosmotrope.[53]

It is reasonable to characterize anions according to the same scheme. Of the halides, F^- is the only cosmotrope, while the others are chaotropic (although Cl^- is borderline). We apply the multiple-charge rule to assume that oxide and tartrate are cosmotropic. Of the complex anions, known cosmotropes (with positive *B*-coefficient) include hydroxide, the carbonates, phosphates, sulfate, and carboxylates (formate and acetate). The *B*-coefficient for $HAsO_4^{2-}$ is not available, so we assume it to be cosmotropic following the other arsenates (and HPO_4^{2-}). Complex chaotropes include nitrate and perchlorate. Ammonium is also a chaotrope, while tetramethylammonium is cosmotropic. The status of cyanide and thiocyanate is uncertain; with both positive and negative *B*-coefficients reported, we accept the negative estimates and take them to be chaotropic.[14,51] It is curious that tetramethylammonium is indicated by the *B*-coefficients to be cosmotropic, because this ion is relatively large with large polarizability. Comparable singly charged ions such as choline are more commonly chaotropic.[54]

To summarize, for the purposes of estimating electrostatic (not dispersion) energies in solution, chaotropic ions with a weakly bound solvation shell should use ionic volumes and radii as listed in Tables 1 and 2 (for the metal cations, exclusive volumes without overlap should be used rather than intrinsic Gaussian volumes). For cosmotropic ions with tightly bound hydration shells, solvated ionic volumes should be used. Solvated ionic volumes and mean spherical radii for known cosmotropes are listed in Table 3.

The questions of solvated ion radius raised here are relevant only in regards to electrostatic energies, eq 9 (or eq 1 for chaotropic metal cations). Dispersion energies (e.g., eq 3) have been explicitly formulated using the intrinsic Gaussian charge distribution and should use Gaussian radii a_g from Tables 1 and 2.

There ought not to be an exact match between the experimental solvation energies and theoretical electrostatic energies present in Figure 3 because the experimental energies include both electrostatic and dispersion contributions. We will consider the theoretical contribution of the latter in a separate paper presenting ab initio calculations of dynamic polarizabilities.[37]

Finally, we note that interactions between the ion and its hydration shell involve quantum mechanical dispersion interactions as well as purely electrostatic interactions. These quantum effects were simplified in the estimates of solvated cosmotropic ion sizes given in Table 3. Equivalent hard-sphere radii of ion and water were used to provide an approximation of the electron cloud overlap between ion and hydration shell. However, we also expect that the ionic polarizabilities responsible for dispersion interactions (cf., eq 3) for ions in vacuo will differ from solvated ions in solution. That is, when applying eq 3 to calculate the dispersion energy of a solvated ion, not only will a different radius apply for the solvated ion, but also a different dynamic polarizability $\alpha(i\omega)$ for the solvated system will be required. The hydration shell modifies the polarizability of the ion due to the interaction between the ionic electron cloud and the solvent molecules in the hydration shell. Likewise, the ion will affect the polarization response of those solvent molecules.

TABLE 3: Solvated Molar Volumes and Mean Solvated Spherical Radii, Used for Electrostatic Energies, for a Selection of Cosmotropic Ions with Tightly Bound Hydration Shells[a]

ion	a_g (Å)	V_{solv} (cm^3/mol)	a_s (Å)
F^-	2.05	29.1	2.26
Li^+	1.42	9.6	1.56
Na^+	1.64	14.9	1.81
Be^{2+}	1.32	7.7	1.45
Mg^{2+}	1.54	12.3	1.69
Ca^{2+}	1.83	20.7	2.02
Sr^{2+}	2.00	26.7	2.19
Ba^{2+}	2.25	38.0	2.47
oxide O^{2-}	2.98	89.1	3.28
hydronium H_3O^+	2.01	27.3	2.21
hydroxide	2.30	40.6	2.53
carbonate	3.17	106.9	3.49
bicarbonate	3.09	99.2	3.40
sulfate	3.33	124.1	3.66
hydrogen sulfate	3.26	116.4	3.59
phosphate	3.43	135.8	3.78
hydrogen phosphate	3.36	127.1	3.69
dihydrogen phosphate	3.30	120.7	3.63
arsenate	3.48	141.1	3.82
hydrogen arsenate	3.42	134.4	3.76
dihydrogen arsenate	3.37	128.4	3.71
formate	3.00	90.6	3.30
acetate	3.23	113.3	3.55
tartrate	3.79	182.8	4.17
citrate	4.05	223.5	4.46
tetramethylammonium	3.51	145.2	3.86

[a] a_g is the solvated gaussian radius; a_s is the equivalent solvated hard-sphere radius. Quantities obtained by adding the hard-sphere radii of water to the bare ion, $a_s^{solv} = a_s^{ion} + a_s^{water}$. Cosmotropic ions are identified as those with a positive Jones−Dole *B*-coefficient.[14,51]

Moreover, returning to the electrostatic solvation energy U_{solv}, we saw that the use of a hydrated cavity radius for cations brought the energy in line with experimental values. However, because $U_{solv} = U_s[\varepsilon_0] - U_s[\text{vac}]$, it is clearly inadequate to take the same hydrated cavity radius used for the self-energy $U_s[\varepsilon_0]$ in solution and apply it to the self-energy $U_s[\text{vac}]$ in vacuum. It makes sense to only use the smaller intrinsic ionic radius to describe the self-energy in vacuum, which leads to the severe overestimate in solvation energy seen in cations before accounting for cavity radii. An inconsistency in the use of the ionic radius for electrostatic interactions therefore remains. While accounting for solvent spatial structure[55−58] will partially correct the discrepancy, it seems likely an additional hydration energy term, comparing the naked ion in vacuum against the solvated ion cluster in vacuum, will also be required.

Thus, a full theoretical description of solvation energies requires a consistent description of the solvated cluster, determining not only ionic, or solvated cluster, volumes, and radii, but also calculating polarizabilities of the solvated clusters taken as a whole. The final result is a balance between the competing effects of larger cluster size (which decreases electrostatic and dispersion self-energies) and cluster polarizability (which will strengthen the dispersion self-energy for ions whose intrinsic polarizability is less than that of water). From the ambiguity discussed above concerning the proper radius of ionic cations, it seems clear that a simple, bare ion description of solvation effects will never fully reproduce experimental solvation energies. Existing studies[38,59] have focused on separating the static

TABLE 4: Static Anisotropic Polarizabilities α_x, α_y, α_z, and Anisotropic Gaussian Radii a_x, a_y, a_z for Nonspherical Ions and Molecules

name	α_x (Å^3)	α_y (Å^3)	α_z (Å^3)	a_x (Å)	a_y (Å)	a_z (Å)
hydronium H_3O^+	0.948	0.948	0.750	1.05	1.05	0.83
hydroxide	2.496	2.871	2.871	1.15	1.32	1.32
nitrate	4.618	4.618	2.787	2.38	2.38	1.44
cyanide	3.518	3.518	4.709	1.71	1.71	2.29
thiocyanate	6.154	6.153	9.977	1.85	1.85	3.01
triflate $CF_3SO_3^-$	6.299	6.299	6.609	2.40	2.40	2.52
chlorate	6.457	6.457	3.551	2.61	2.61	1.43
carbonate	6.601	6.601	4.928	2.35	2.35	1.76
hydrogen carbonate	4.774	4.517	3.238	2.38	2.25	1.62
hydrogen sulfate	5.162	5.086	5.019	2.26	2.22	2.19
hydrogen phosphate	6.994	6.811	6.732	2.37	2.31	2.28
dihydrogen phosphate	5.330	5.392	5.687	2.21	2.23	2.36
hydrogen arsenate	8.108	7.993	7.736	2.43	2.40	2.32
dihydrogen arsenate	6.737	6.223	6.173	2.47	2.28	2.26
cacodylate	9.114	10.287	9.497	2.41	2.72	2.51
formate	4.688	4.188	2.934	2.38	2.13	1.49
acetate	6.157	6.169	4.496	2.44	2.44	1.78
tartrate	12.320	11.391	9.692	3.06	2.83	2.41
citrate	17.668	15.577	14.907	3.33	2.94	2.81
water	1.315	1.222	1.152	1.11	1.03	0.97
ammonia	1.846	1.846	1.947	1.20	1.20	1.27
formamide	4.469	3.651	2.723	2.48	2.03	1.51
ethanolamine$-H^+$	5.840	4.818	4.468	2.59	2.14	1.98
glycine±	6.203	6.665	4.568	2.44	2.63	1.80
choline	10.654	9.206	9.003	2.98	2.58	2.52
CO_2	1.723	1.723	3.359	1.25	1.25	2.45
O_2 (triplet)	1.026	1.026	2.331	0.90	0.90	2.05
O_2 (singlet)	1.106	1.094	2.078	0.96	0.95	1.81
N_2	1.417	1.417	2.117	1.12	1.12	1.67

polarizability of the ion from within the solvated cluster but have not studied the polarizability of the solvated cluster as a single entity, thereby omitting effects of the ion on the solvation shell.

Rather, we expect greater success working with solvated ion clusters, with dispersion energies arising from the dynamic polarizabilities of the solvated clusters taken as a whole. This will be the subject of future work.

9. Nonspherical Ions and Molecules

The spherical Gaussian charge distribution of eq 5 may be generalized to the nonspherical case using an ellipsoidal distribution,

$$\rho(\vec{r}) = \frac{1}{V}\exp\left\{-\left[\left(\frac{x}{a_x}\right)^2 + \left(\frac{y}{a_y}\right)^2 + \left(\frac{z}{a_z}\right)^2\right]\right\} \qquad (10)$$

with anisotropic Gaussian radii a_x, a_y, and a_z. In this case, the ionic volume is $V = \pi(\sqrt{\pi})^{1/2}a_x a_y a_z$.

We determine the aspect ratio of the ellipsoid using the nonisotropic polarizability tensor, taking only the diagonal elements α_x, α_y, α_z (assuming off-diagonal elements are zero). If the aspect ratio is preserved, then the size of the nonspherical ion is determined by a single parameter, the girth g, relating the anisotropic Gaussian radii to the polarizability elements such that

$$a_x = \frac{\alpha_x}{\alpha_0}g,\ a_y = \frac{\alpha_y}{\alpha_0}g,\ a_z = \frac{\alpha_z}{\alpha_0}g \qquad (11)$$

where α_0 is the mean isotropic static polarizability, $\alpha_0 = (\alpha_x + \alpha_y + \alpha_z)/3$. The girth g is the mean isotropic (spherical) radius with dimensions of length and equals the spherical radius when the ion or molecule is spherical.

The exclusive volume V_{ex} of section 2 remains the same, inscribed by an isodensity surface at $\rho_0 = 0.001$ electron/Bohr^3. The corresponding exclusive ellipsoid has anisotropic exclusive radii $a_i^{ex} = g_{ex}\alpha_i/\alpha_0$, $i = x, y, z$. The exclusive girth g_{ex} is determined from the ab initio exclusive volume, which for a hard spheroid equals $V_{ex} = 4\pi a_x^{ex}a_y^{ex}a_z^{ex}/3 = 4\pi\alpha_x\alpha_y\alpha_z g_{ex}^3/3\alpha_0^3$.

Let us consider the extremal points on the exclusive surface, $\vec{r}_1 = (a_x^{ex}, 0, 0)$, $\vec{r}_2 = (0, a_y^{ex}, 0)$, $\vec{r}_3 = (0, 0, a_z^{ex})$. At each of these points, $\rho(\vec{r}_i) = \rho_0$. For instance, for $\vec{r}_1$,

$$\rho(\vec{r}_1) = \frac{\exp\{-[(a_x^{ex}/a_x)^2 + 0 + 0]\}}{\pi\sqrt{\pi}a_x a_y a_z} = \frac{\alpha_0^3\exp\{-(g_{ex}/g)^2\}}{\pi\sqrt{\pi}\alpha_x\alpha_y\alpha_z g^3} = \rho_0 \qquad (12)$$

The same equation in g appears for $\vec{r}_2$ and $\vec{r}_3$. Thus, we obtain a transcendental equality in g, similar to eq 7 for the spherical case. The solution is the same apart from the introduction of the polarizability parameters α_i (thus the spherical problem of section 4 is a special case of the nonspherical problem where the polarizability terms cancel). Solving for g gives us the anisotropic Gaussian radii a_x, a_y, a_z.

As before, there may be two solutions for g close to g_{ex}; we accept the smaller solution. We allow the exclusive volume to relax within its error bars in seeking a solution to the equality. Where there is no solution, we accept the least-squares solution varying g to minimize $[\rho(g) - \rho_0]^2$.

The anisotropic polarizabilities and corresponding anisotropic Gaussian radii for nonspherical ions and molecules are given in Table 4. These are properties of the bare ions and molecules, without consideration of hydration shells. Again, static polarizability tensors were calculated at the Hartree−Fock level of theory using aug-cc-pVQZ and other basis sets used in calculations of dynamic polarizabilities.[37] Note that, because the

geometric mean of the three anisotopic polarizability tensor elements is nearly equal to the arithmetic mean, the ellipsoidal Gaussian volumes V_g are the same (within the given precision) as those calculated using the spherical approximation and are already listed in Table 2.

10. Conclusion

Ab initio exclusive volumes have been calculated for a range of ions and molecules and used to derive Gaussian radii for a spatially diffuse model of the ion or molecule's charge distribution. These Gaussian radii have immediate application in existing theories of dispersion interactions, which have been developed using polarizabilities with the same spatial distribution. The corresponding form for the electrostatic self-energy has also been derived.

Together with the calculation of ab initio dynamic polarizabilities of the same ions and molecules,[37] this paves the way toward a more quantitative accurately theoretical description of ion-specific effects. The ionic radii presented in this Article are intended to play a role as one of several input parameters, alongside ionic charge, ionic polarizability, and solvent dielectric function, which together give a complete description of electrolyte properties, including both electrostatic and dispersion interactions. Preliminary calculations indicate that our radii (and dynamic polarizabilities), including the distinction drawn between cosmotropic and chaotropic ions, are successful at reproducing the Hofmeister series of alkali halides, providing quantitatively reasonable activity coefficients without further fitting of ionic radii.

Analysis of electrostatic solvation energies indicates there are still open questions with regard to the effect of an ion's solvation shell. The solvation shell does not appear to be important for chaotropic ions, where it is weakly bound, but must be included as part of the solvation complex of cosmotropic ions. The free energy of solvated ion clusters and periodic systems with explicit water molecules has been studied via ab initio Car−Parrinello molecular dynamics,[43−48,60,61] demonstrating that the local solvation environment must indeed be included to gain accurate solvation energies. We suggest it may be appropriate to consider the solvated ion cluster calculated in these kind of studies as the basic unit entering into theoretical continuum models, with ion polarizability and ion radius referring to that of the solvated ion rather than the bare ion. By taking electrostatic and dispersion interactions together in this hydrated ion model, along with solvent−solvent correlations via a k-dependent description of the solvent,[55−58] a softer potential should be obtained that accounts for ion−solvent as well as ion−ion interactions. This leads to a kind of generalized Gurney potential with interaction between ions being mediated by overlap of their hydration shells and should provide a framework for distinguishing between hard and soft ions.

Another important factor in need of theoretical application is the effect of ionic anisotropy. To that end, we have calculated anisotropic Gaussian radii for nonspherical ions and molecules on the basis of their nonisotropic static polarizability tensors. We expect the question of anisotropy will prove particularly pertinent to surface and interface phenomena, where the interaction of a flat molecule at a surface will be markedly different when aligned perpendicular to or parallel with the surface.

Both of the conditions discussed here of a hydrated and an anisotropic ion meet in the example of the hydroxide ion. There is experimental evidence of specific adsorption of hydroxide ions at the air−water interface;[62] yet molecular dynamic simulations predict a depletion of hydroxide ions at the surface.[63] The hydrated hydroxide ion $[OH^{\bullet}(H_2O)_3]^-$ is a near-planar tetrahedral complex.[61,64,65] We suggest that MD simulations treating the hydrated hydroxide ion as a single entity may have greater success in predicting surface adsorption.

References and Notes

(1) Ninham, B.; Yaminsky, V. *Langmuir* **1997**, *13*, 2097–2108.
(2) Kunz, W.; Lo Nostro, P.; Ninham, B. W. *Curr. Opin. Colloid Interface Sci.* **2004**, *9*, 1–18.
(3) Bostrom, M.; Williams, D.; Ninham, B. *Langmuir* **2001**, *17*, 4475–4478.
(4) Cheng, J.; Vecitis, C. D.; Hoffmann, M. R.; Colussi, A. J. *J. Phys. Chem. B* **2006**, *110*, 25598–25602.
(5) Cheng, J.; Hoffmann, M. R.; Colussi, A. J. *J. Phys. Chem. B* **2008**, *112*, 7157–7161.
(6) Hummer, G.; Pratt, L.; Garcia, A. *J. Phys. Chem. A* **1998**, *102*, 7885–7895.
(7) Kunz, W.; Belloni, L.; Bernard, O.; Ninham, B. *J. Phys. Chem. B* **2004**, *108*, 2398–2404.
(8) Blum, L.; Fawcett, W. R. *J. Phys. Chem.* **1992**, *96*, 408–414.
(9) Pauling, L. *J. Am. Chem. Soc.* **1927**, *49*, 765–790.
(10) Gourary, B. S.; Adrian, F. J. In *Solid State Physics*; Seitz, F., Turnbull, D., Eds.; Academic Press Inc.: New York, 1960; Vol. 10, p 128.
(11) Marcus, Y. *Chem. Rev.* **1988**, *88*, 1475–1498.
(12) Johnson, O. *Inorg. Chem.* **1973**, *12*, 780–785.
(13) Rashin, A. A.; Honig, B. *J. Phys. Chem.* **1985**, *89*, 5588–5593.
(14) Collins, K. *Biophys. Chem.* **2006**, *119*, 271–281.
(15) Collins, K. D. *Methods* **2004**, *34*, 300–311.
(16) Jungwirth, P.; Tobias, D. *J. Phys. Chem. A* **2002**, *106*, 379–383.
(17) Dorsett, H.; Watts, R.; Xantheas, S. *J. Phys. Chem. A* **1999**, *103*, 3351–3355.
(18) Mahanty, J.; Ninham, B. W. *Dispersion Forces*; Academic Press: London, 1976.
(19) Mahanty, J. *Nuovo Cimento B* **1974**, *22*, 110.
(20) Mahanty, J.; Richardson, D. D. *J. Phys. C: Solid State Phys.* **1975**, *8*, 1322–1331.
(21) Mahanty, J.; Ninham, B. W. *Faraday Discuss. Chem. Soc.* **1975**, *59*, 13–21.
(22) Mahanty, J.; Ninham, B. W. *J. Chem. Phys.* **1973**, *59*, 6157–6162.
(23) Netz, R. R. *Curr. Opin. Colloid Interface Sci.* **2004**, *9*, 192–197.
(24) Richardson, D. D. *J. Phys. A: Math. Gen.* **1975**, *8*, 1828–1841.
(25) Schmidt, P.; McKinley, J. *J. Chem. Soc., Faraday Trans. 2* **1976**, *72*, 143–170.
(26) Paranjape, V. V.; Mahanty, J. *Phys. Rev. A* **1979**, *19*, 2466–2469.
(27) Lu, J. X.; Marlow, W. H. *Phys. Rev. A* **1995**, *52*, 2141–2154.
(28) Alfridsson, M.; Ninham, B.; Wall, S. *Langmuir* **2000**, *16*, 10087–10091.
(29) Kim, H.; Tuite, E.; Nordén, B.; Ninham, B. *Eur. Phys. J. E* **2001**, *4*, 411–417.
(30) Bunkin, N. F.; Kochergin, A. V.; Lobeyev, A. V.; Ninham, B. W.; Vinogradova, O. I. *Colloids Surf., A: Physicochem. Eng. Aspects* **1996**, *110*, 207–212.
(31) Craig, V.; Ninham, B.; Pashley, R. *Langmuir* **1999**, *15*, 1562–1569.
(32) Ninham, B. *Prog. Colloid Polym. Sci.* **2006**, *133*, 65–73.
(33) Born, M. *Z. Phys.* **1920**, *1*, 45–49.
(34) Frisch, M. J.; Trucks, G. W.; Schlegel, H. B.; Scuseria, G. E.; Robb, M. A.; Cheeseman, J. R.; Montgomery, J. A., Jr.; Vreven, T.; Kudin, K. N.; Burant, J. C.; Millam, J. M.; Iyengar, S. S.; Tomasi, J.; Barone, V.; Mennucci, B.; Cossi, M.; Scalmani, G.; Rega, N.; Petersson, G. A.; Nakatsuji, H.; Hada, M.; Ehara, M.; Toyota, K.; Fukuda, R.; Hasegawa, J.; Ishida, M.; Nakajima, T.; Honda, Y.; Kitao, O.; Nakai, H.; Klene, M.; Li, X.; Knox, J. E.; Hratchian, H. P.; Cross, J. B.; Bakken, V.; Adamo, C.; Jaramillo, J.; Gomperts, R.; Stratmann, R. E.; Yazyev, O.; Austin, A. J.; Cammi, R.; Pomelli, C.; Ochterski, J. W.; Ayala, P. Y.; Morokuma, K.; Voth, G. A.; Salvador, P.; Dannenberg, J. J.; Zakrzewski, V. G.; Dapprich, S.; Daniels, A. D.; Strain, M. C.; Farkas, O.; Malick, D. K.; Rabuck, A. D.; Raghavachari, K.; Foresman, J. B.; Ortiz, J. V.; Cui, Q.; Baboul, A. G.; Clifford, S.; Cioslowski, J.; Stefanov, B. B.; Liu, G.; Liashenko, A.; Piskorz, P.; Komaromi, I.; Martin, R. L.; Fox, D. J.; Keith, T.; Al-Laham, M. A.; Peng, C. Y.; Nanayakkara, A.; Challacombe, M.; Gill, P. M. W.; Johnson, B.; Chen, W.; Wong, M. W.; Gonzalez, C.; Pople, J. A. Gaussian 03, revision C.02; Gaussian, Inc.: Wallingford, CT, 2004.
(35) Thom, H.; Dunning, J. *J. Chem. Phys.* **1989**, *90*, 1007–1023.
(36) Woon, D. E.; Thom, H.; Dunning, J. *J. Chem. Phys.* **1993**, *98*, 1358–1371.
(37) Parsons, D. F.; Ninham, B. W., submitted for publication.
(38) Serr, A.; Netz, R. R. *Int. J. Quantum Chem.* **2006**, *106*, 2960–2974.
(39) Lim, I. S.; Schwerdtfeger, P.; Metz, B.; Stoll, H. *J. Chem. Phys.* **2005**, *122*, 104103.

(40) Lim, I. S.; Stoll, H.; Schwerdtfeger, P. *J. Chem. Phys.* **2006**, *124*, 034107.
(41) Adamovic, I.; Gordon, M. *Mol. Phys.* **2005**, *103*, 379–387.
(42) Woon, D. E.; Thom, H.; Dunning, J. *J. Chem. Phys.* **1994**, *100*, 2975–2988.
(43) Grabowski, P.; Riccardi, D.; Gomez, M.; Asthagiri, D.; Pratt, L. *J. Phys. Chem. A* **2002**, *106*, 9145–9148.
(44) Rempe, S.; Pratt, L.; Hummer, G.; Kress, J.; Martin, R.; Redondo, A. *J. Am. Chem. Soc.* **2000**, *122*, 966–967.
(45) Asthagiri, D.; Pratt, L. R.; Kress, J. D.; Gomez, M. A. *Proc. Natl. Acad. Sci. U.S.A.* **2004**, *101*, 7229–7233.
(46) Asthagiri, D.; Pratt, L. R. *Chem. Phys. Lett.* **2003**, *371*, 613–619.
(47) Geissler, P. L.; Dellago, C.; Chandler, D.; Hutter, J.; Parrinello, M. *Science* **2001**, *291*, 2121–2124.
(48) Izvekov, S.; Voth, G. A. *J. Chem. Phys.* **2005**, *123*, 044505.
(49) Lide, D. R., Ed. *CRC Handbook of Chemistry and Physics*, 84th ed.; CRC Press: New York, 2004.
(50) Collins, K. D. *Biophys. J.* **1997**, *72*, 65–76.
(51) Jenkins, H. D. B.; Marcus, Y. *Chem. Rev.* **1995**, *95*, 2695–2724.
(52) Salabat, A.; Shamshiri, L.; Sahrakar, F. *J. Mol. Liq.* **2005**, *118*, 67–70.
(53) Olah, S.; Kremmer, T.; Boldizsar, M. *J. Chromatogr., B* **2000**, *744*, 73–79.
(54) Vrbka, L.; Jungwirth, P.; Bauduin, P.; Touraud, D.; Kunz, W. *J. Phys. Chem. B* **2006**, *110*, 7036–7043.
(55) Kornyshev, A. A. *J. Chem. Soc., Faraday Trans. 2* **1983**, *79*, 651–661.
(56) Basilevsky, M. V.; Parsons, D. F. *J. Chem. Phys.* **1998**, *108*, 9107–9113.
(57) Basilevsky, M. V.; Parsons, D. F. *J. Chem. Phys.* **1998**, *108*, 9114–9123.
(58) Parsons, D. F.; Ninham, B. W, in preparation.
(59) Jungwirth, P.; Curtis, J. E.; Tobias, D. J. *Chem. Phys. Lett.* **2003**, *367*, 704–710.
(60) Tobias, D. J.; Jungwirth, P.; Parrinello, M. *J. Chem. Phys.* **2001**, *114*, 7036–7044.
(61) Tuckerman, M. E.; Marx, D.; Parrinello, M. *Nature* **2002**, *417*, 925–929.
(62) Karraker, K. A.; Radke, C. J. *Adv. Colloid Interface Sci.* **2002**, *96*, 231–264.
(63) Jungwirth, P.; Tobias, D. *Chem. Rev.* **2006**, *106*, 1259–1281.
(64) Robertson, W. H.; Diken, E. G.; Price, E. A.; Shin, J.-W.; Johnson, M. A. *Science* **2003**, *299*, 1367–1372.
(65) Cappa, C.; Smith, J.; Messer, B.; Cohen, R.; Saykally, R. *J. Phys. Chem. A* **2007**, *111*, 4776–4785.

JP802984B